Eur Spine J (2012) 21 (Suppl 6):S860–S867
DOI 10.1007/s00586-012-2164-8

ORIGINAL ARTICLE

Intraoperative determination of the load–displacement behavior of scoliotic spinal motion segments: preliminary clinical results

Christoph Reutlinger · Carol Hasler · Klaus Scheffler · Philippe Büchler

Received: 16 January 2012 / Accepted: 18 January 2012 / Published online: 8 February 2012

Abstract
Introduction Spinal fusion is a widely and successfully performed strategy for the treatment of spinal deformities and degenerative diseases. The general approach has been to stabilize the spine with implants so that a solid bony fusion between the vertebrae can develop. However, new implant designs have emerged that aim at preservation or restoration of the motion of the spinal segment. In addition to static, load sharing principles, these designs also require a profound knowledge of kinematic and dynamic properties to properly characterise the in vivo performance of the implants.
Methods To address this, an apparatus was developed that enables the intraoperative determination of the load–displacement behavior of spinal motion segments. The apparatus consists of a sensor-equipped distractor to measure the applied force between the transverse processes, and an optoelectronic camera to track the motion of vertebrae and the distractor. In this intraoperative trial, measurements from two patients with adolescent idiopathic scoliosis with right thoracic curves were made at four motion segments each.
Results At a lateral bending moment of 5 N m, the mean flexibility of all eight motion segments was 0.18 ± 0.08°/N m on the convex side and 0.24 ± 0.11°/N m on the concave side.
Discussion The results agree with published data obtained from cadaver studies with and without axial preload. Intraoperatively acquired data with this method may serve as an input for mathematical models and contribute to the development of new implants and treatment strategies.

Keywords Scoliosis · Motion segment · Spine · Mechanical properties · In vivo measurements

Introduction

Nonfusion operative methods for the treatment of degenerative spinal diseases and deformities have tremendous potential to increase the patient quality of life. In addition to the fact that motion is preserved or restored, a natural load transfer to the adjacent segments is sustained. This is important, as clinical experience shows that fusion of motion segments frequently can entail adjacent level degeneration [8, 10]. However, nonfusion implants are challenging, particularly for the treatment of spinal deformities, in which several segments are commonly affected. Concerning the design of growing implants to treat adolescent idiopathic scoliosis, crucial issues are the required force to distract the spine and the most effective positioning of the implant. Thus, a better understanding of the mechanical properties of healthy and pathological motion segments is essential.

Both in vitro and in vivo measurement techniques are necessary to gain a thorough understanding of biomechanical structures. In vitro measurements performed on spinal loading simulators have become the standard technique to investigate spinal biomechanics and implant

C. Reutlinger (✉) · P. Büchler
Institute for Surgical Technology and Biomechanics, University of Bern, Bern, Switzerland
e-mail: christoph.reutlinger@istb.unibe.ch

C. Hasler
Orthopaedic Department, University Children's Hospital, Basel, Switzerland

K. Scheffler
Department of Neuroimaging and MR Physics, Medical Faculty, University of Tübingen, Tübingen, Germany

performance (e.g., [6, 25]). While experiments can be performed under well-defined and controlled conditions, questions about the limitations of testing an isolated specimen remain. In vivo experiments allow measurements in a physiological environment of patients of the desired age with the pathology of interest. On the other hand, due to restricted anatomical accessibility and safety reasons, in vivo measurements allow limited loading scenarios and mechanical data cannot be acquired up to the failure limit.

Due to the high prevalence of low back pain, experimental studies have been conducted predominantly on the lumbar spine. Moment–angle relations were investigated by Guan et al. [11], Oxland et al. [17], Panjabi et al. [20] and Yamamoto et al. [26]. Experiments to examine the influence of functional spinal structures have also been performed. Heuer et al. [13, 14] consecutively removed ligaments, facet capsules, joints and the nucleus, and measured the moment–angle relation after each step. A few experimental studies are available that have investigated the mechanical properties of cadaveric human thoracic specimens. Panjabi et al. [18] measured the three-dimensional load–displacement behavior of single motion segments of the entire thoracic spine. Busscher et al. [2] tested multilevel segments of the thoracic and lumbar part of the spine by applying pure moments up to 4 N m in the main anatomical directions. Sran et al. [23] used specimens from T5 to T8 and applied moments of 4 N m.

Some studies exist, in which in vivo intraoperative data were acquired from degenerated lumbar segments [1, 5, 12]. In each of these studies, measurements were performed with spinal distractors between the spinous processes to quantify the instability of the motion segment. However, because force–displacement relations were determined, the data could not be compared to in vitro experiments, in which moment–angle relations are commonly measured.

Patient-specific material properties of spinal segments were evaluated with a parameter identification of mathematical models. Studies solving this inverse problem for scoliotic spines using radiographs in an upright and bent or elongated position have been reported. Ghista et al. [9] used a two-dimensional mathematical representation of the spine, while Petit et al. [21] and recently Lafon et al. [16] used more detailed, three-dimensional models. An important result of these studies is that published mechanical properties for straight spines cannot adequately reproduce the bent position, while individually adapted parameters resulted in considerable improvement. However, the optimization was based only on the displacement of the vertebrae, and the forces applied to obtain this displacement were not taken into account.

Combining intraoperative distractor measurements with motion tracking gives a complete description of the applied load and the resulting motion on a patient-specific basis. Knowing the magnitude and the orientation of the force vector and the relative motion of the vertebrae, moment–angle relations can be determined. Intraoperatively measured data can thus be compared to existing in vitro studies. Such measurements can be performed anytime posterior surgical access to the spine is chosen.

The concept of using a sensor-equipped distractor and a motion tracking system to determine the flexibility of spinal motion segments has been previously validated [22]. The objective of this study was to obtain intraoperative measurements. Patients with adolescent idiopathic scoliosis offer the possibility of performing measurements at multiple motion segments, as the spine is exposed across several levels. Furthermore, the mechanical properties of motion segments from adolescent, deformed spines are scarcely available.

Materials and methods

Distraction-based kinematic measurement setup

To determine the three-dimensional load–displacement behavior of spinal motion segments, an apparatus was developed that combined optoelectronic motion tracking and surgical instrumentation. A standard Synthes distraction forceps used in lumbar fusion surgeries was equipped with two strain gauges (1-LY61-3/120, HBM, Volketswil, Switzerland), which were arranged in a half-Wheatstone bridge configuration. The applied force was determined based on the bending moment applied through the handles. The strain gauges were calibrated to measure the force applied at the tips and a standard Hall effect sensor was included, which was calibrated to measure the opening of the distractor tips (Fig. 1a). These modifications were developed jointly with the University of Applied Sciences in Biel, Switzerland and have been published by Krenn et al. [15]. Both the distractor and the two vertebrae of a motion segment were tracked with an optoelectronic camera (Optotrack 3020, Northern Digital Inc., Waterloo, Canada). The dynamic reference bases to track the vertebrae consisted of four light-emitting diodes (LEDs). The distractor was equipped with two cruciform marker shields, each with four LEDs to guarantee sufficient camera visibility when using it on both sides of the curved spine. Based on the recorded motion of the vertebrae, the axis of rotation was determined [3]. As both the orientation and the magnitude of the force vector were measured, the applied moment could be computed. This approach was validated with measurements performed on a spinal loading simulator using lumbar ovine specimens. Bending stiffness was chosen to be the comparative measure. Up to

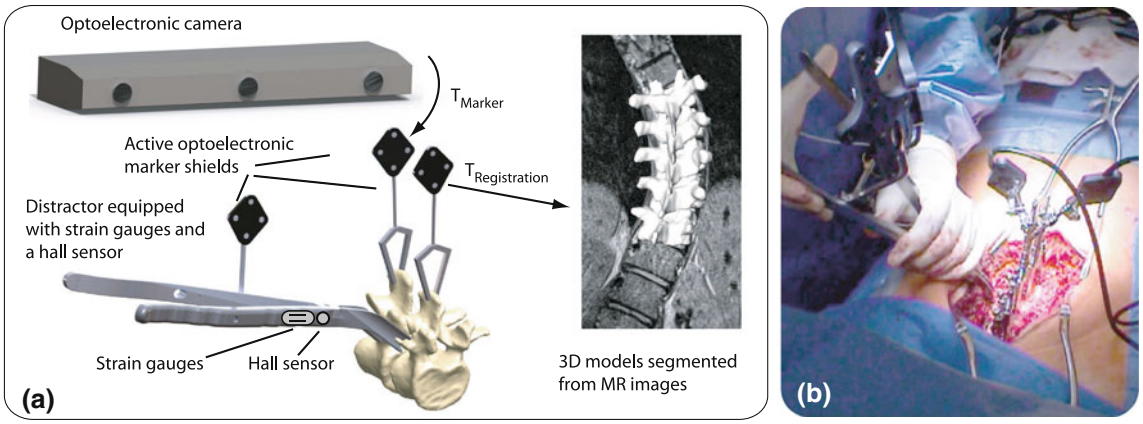

Fig. 1 **a** Systematic sketch with the main components of the measurement concept: Optotrack 3020 camera (Northern Digital Inc., Waterloo, Canada) for optical tracking of distractor and vertebrae, instrumented distractor with strain gauges to measure the force applied at the tips and a Hall effect sensor to measure the opening of the tips and **b** intraoperative measurement

applied loads of 5 N m, the stiffness determined with our apparatus was within a range of ±15% of the stiffness measured with the spinal loading simulator. A detailed description of the apparatus and its validation has been recently published in Reutlinger et al. [22].

The 3D models, required for the tracking of the vertebrae, were based on CT images in the validation study, but segmented from MR images for the intraoperative measurements. To assess the error associated with the segmentation based on the two image modalities, CT and MR images of nine ovine lumbar vertebrae were acquired. Surface models of the vertebrae were segmented from both modalities and after a rigid registration the distance map of the surfaces was determined. The greatest differences were at the tips of the transverse and spinous processes and at the facet joints. Along the surfaces of the transverse processes, the lamina and the spinous process, the difference was <0.5 mm. The overall distance error of all nine vertebrae was 0.57 ± 0.5 mm.

Intraoperative measurements

Intraoperative measurements were approved for five patients with adolescent idiopathic scoliosis with right thoracic curves by the ethical committee of the University Children's Hospital Basel, Switzerland. Due to soft- and hardware adaptations and changes in the intraoperative workflow, only the last two measurements could be performed with an identical setup. The results of the measurements performed for these two patients (Table 1) are presented here.

MR images were acquired with a T1-weighted sequence on a 1.5-T device (MAGNETOM Avanto, Siemens AG, Erlangen, Germany). The in-plane resolution was 1×1 mm^2 and the slice thickness was 1 mm. 3D models of the vertebrae, required for navigation, were created by manually segmenting the MR images using Amira (Visage Imaging, Richmond, Australia). The sensors of the distractor were calibrated and the distractor was then sterilized in hydrogen peroxide plasma at about 50°C for 45 min. The patients were under general anesthesia and in a prone position. After a skin incision, the thoracic spine was exposed subperiosteally to the tips of the transverse processes in a standard way. All ligaments were preserved, except for the intertransverse ligament, where a small subperiosteal incision was made to place the distractor.

Table 1 Patient information

	Patient 1	Patient 2
Sex	Female	Female
Age at surgery (years)	12	17
Cobb angle (°)	48	65
Apex	T08	T09

The workflow for the intraoperative measurements was as follows: first, alligator clamps were mounted to the spinous processes of the five vertebrae around the apex of the curvature. Dynamic reference bases were then attached to the alligator clamps at the two most cranial, instrumented vertebrae. In order to track the motion of the vertebrae, the transformation between the 3D models of the vertebrae in the image coordinate system and the dynamic reference base had to be established. This process, called registration, was performed using paired points and surface matching. Three paired points were defined at the tips of the spinous process and the transverse processes. A total of 30 points were digitized for the surface matching along the transverse processes, the lamina and the spinous process. The distractor was placed in the incision between the transverse process, and the force was applied manually by the surgeon (Fig. 1b). A maximum force of 200 N was

applied at a rate of about 0.2 Hz. Four load cycles were performed at each side of the curve. In order to continue, the dynamic reference base of the superior vertebra was removed and a new reference base was attached to the inferior vertebra of the adjacent motion segment.

Data analysis

Local coordinate systems were defined at the 3D models of the vertebrae in the centre of the midsagittal plane of each endplate in the following way: eight landmarks around the vertebral body were manually selected using Amira (Visage Imaging, Richmond, Australia). The orientation of the local z-axis was defined as the vector connecting landmark 1 and landmark 5 (Fig. 2) which gave a proper local anterior-posterior orientation. With least squares, a plane was fitted through the eight landmarks. The normal of that plane was defined as the local y-axis. The local x-axis was determined as the cross product of the y-axis and the z-axis.

Relative motion was determined as the motion of the superior vertebra with respect to the inferior. Rotations were expressed as Euler angles in an x–y–z sequence (i.e., flexion, axial rotation, lateral bending). In order to determine moment–angle relations, force vector and axis of rotation had to be known. The force vector was defined knowing its orientation from the motion tracking and its magnitude from the signal of the calibrated strain gauges. As the force component perpendicular to the tips of the distractor was measured, frictionless contact between the distractor tips and the soft tissue had to be assumed. The circle-fitting approach of Chang and Pollard [3] was chosen to determine the axis of rotation. The circles were fitted through the trajectories of predefined markers such that the axis of rotation passed through their origin and was perpendicular to the circle area. Seven markers were defined at the transverse and spinous processes and at the anterior portion of the superior endplate (Fig. 2). Knowing a point on the axis of rotation and its orientation, the lever arm could be determined. The moment was computed as the cross product of lever arm and force vector [22]. As the applied force vector generally is not perpendicular to the axis of rotation, the orientation of the moment vector and of the axis of rotation do not coincide, which means that the method is able to describe coupling patterns. Finally, load–displacement data in the lateral bending motion were approximated with the following exponential function:

$$\gamma = a(\mathrm{e}^{bM_z} - c), \tag{1}$$

where the function γ represents the relative angular motion and the argument M_z is the lateral bending moment. Fitting of the constants a, b and c was performed for the loading path of each load cycle using the least squares method (Fig. 3). Four load cycles were performed at each side of the spine. The first load cycle was regarded as preconditioning and the successive three cycles were taken for data analysis.

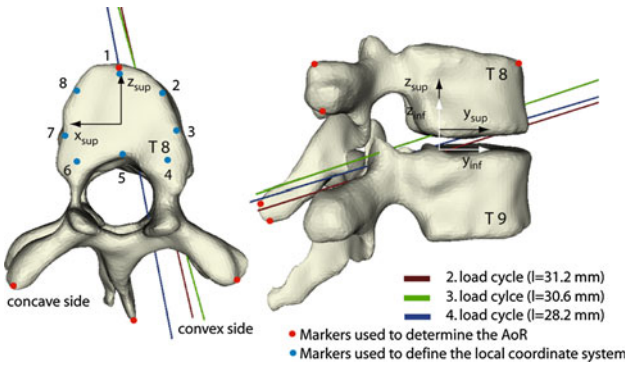

Fig. 2 Determination of the axis of rotation (AoR) and local coordinate systems, patient 2, T08–T09 segment. The force was applied at the concave side. AoRs are shown for load cycles 2–4, l corresponds to the length of the respective lever arm

Results

The registration of the vertebrae and the measurements required about 6 min/motion segment. The total time necessary for the procedure was about 25 min, which accounts for approximately 7% of the time under general anesthesia of 350 min. At the convex side of the T09–T10 segment of patient 1, the force was limited to 120 N, as the surgeon felt the transverse process to fracture. For the T07–T08 segment of patient 1 and the T10–T11 segment of patient 2, no data analysis could be performed. The kinematic data of these motion segments indicated that the marker shields were touched by the surgical team while applying force with the distractor. The mean loading frequency of all load cycles was 0.18 ± 0.04 Hz.

The relative variability of the length of the computed lever arms corresponding to load cycles two to four was determined. The mean relative variability of all measurements was 12.5%. For the T08–T09 segment of patient 2, the axes of rotation of the three load cycles are illustrated (Fig. 2). Moment loading and relative motion for the third load cycle of the T08–T09 segment of patient 2 are displayed in Fig. 3. The fitting of the exponential function to the loading path in the lateral bending motion is also presented. The coefficients of correlation for the fitting were at least $R^2 = 0.92$.

Flexibility and relative motion of all eight motion segments are presented in Fig. 4 for applied moments of 1, 3 and 5 N m. The values are based on the fitting of Eq. 1 to the loading path of the experimental data. Mean values and standard deviation are based on load cycles two to four. Due to the lower distractor force, which was applied at the convex side of the T09–T10 segment of patient 1, the moment

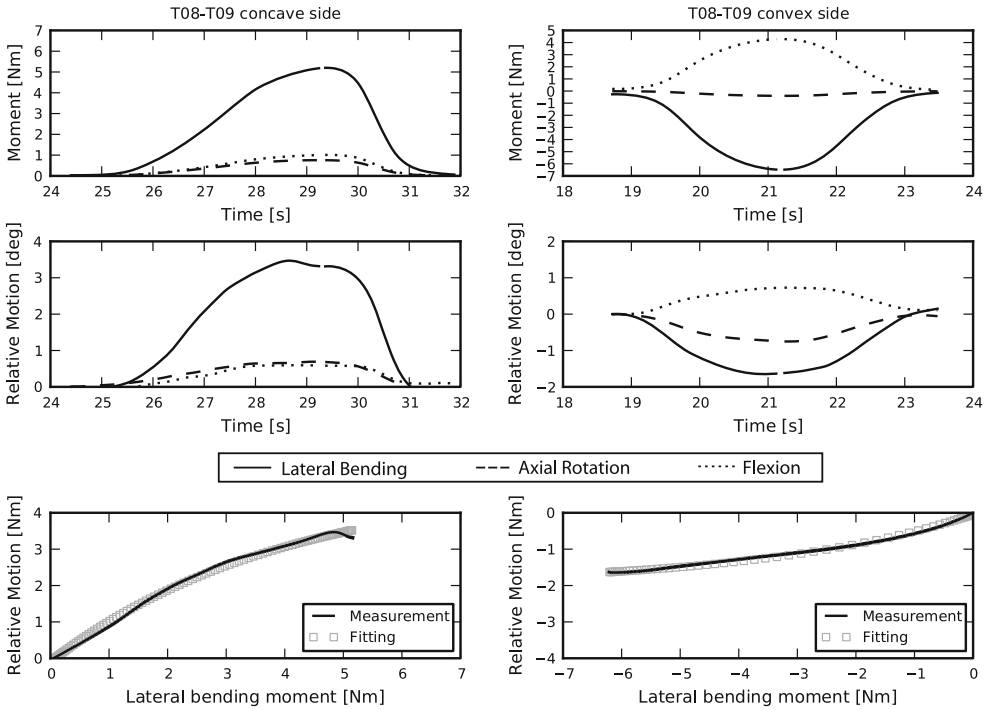

Fig. 3 Example of the analysis of patient 2 for one load cycle of the T08–T09 segment. Rotations are given as Euler angles in a *x*–*y*–*z* sequence (flexion, axial rotation, lateral bending)

was <5 N m. The values for flexibility and relative motion were extrapolated based on the fitting of Eq. 1. On the convex side, flexibility and relative motion were nearly constant along the different levels. The concave side was less uniform and gave slightly higher values. The average flexibility of all motion segments at a bending moment of 5 N m was $0.18 \pm 0.08°$/N m on the convex side and $0.24 \pm 0.11°$/N m on the concave side. The mean respective coefficients of the fitted exponential functions are:

convex side: $a = 2.4°$ $b = 0.21/(\text{N m})$ $c = 1.0$

concave side: $a = -2.6°$ $b = \text{-}0.41/(\text{N m})$ $c = 1.0$.

Since the distractor was placed between the transverse processes, the main component of the moment vector was in the lateral bending direction. Generally, a flexion and, to a lesser extent, a moment causing axial rotation were present (Fig. 3). The combined rotations are also represented by the approximated axis of rotation (Fig. 2). Whereas patient 2 showed a coupling between axial rotation and lateral bending at the convex side (Fig. 3), a coupling pattern could not be observed in patient 1.

Discussion

Posterior surgical access for the treatment of spinal deformities or degenerative diseases permits in vivo intraoperative measurements of the vertebral column. In this trial, forces were applied between the transverse processes with a distractor and the motion of the vertebrae and the distractor was tracked. The combination of force measurement and motion tracking allowed the determination of a moment–angle relation, thus providing intraoperative measurements that can be compared to existing data based on in vitro tests.

The proposed concept was validated from a previous experimental study of lumbar ovine spines employing a spinal loading simulator [22]. For lateral bending moments up to 5 N m, the distractor measurements deviated no more than ±15% from the spinal loading simulator results. The intraoperative study differed from the in vitro validation study in three ways. First, MR images of the adolescent patients were used for diagnosis and planning of the surgery; the geometrical models of the vertebrae for the intraoperative navigation and measurements were thus based on the MR images. Second, there were differences in the support of the motion segments that affected the distribution of the internal moments. In the validation study, the cadaver specimens were mounted to and supported by the spinal loading simulator [7] in a statically determinate manner. This resulted in a situation in which the bearings did not sustain any moment loading. In the intraoperative situation, the adjacent structures also sustain some external loading. This leads to an overestimation of the applied moment and thus to an underestimation of the flexibility of

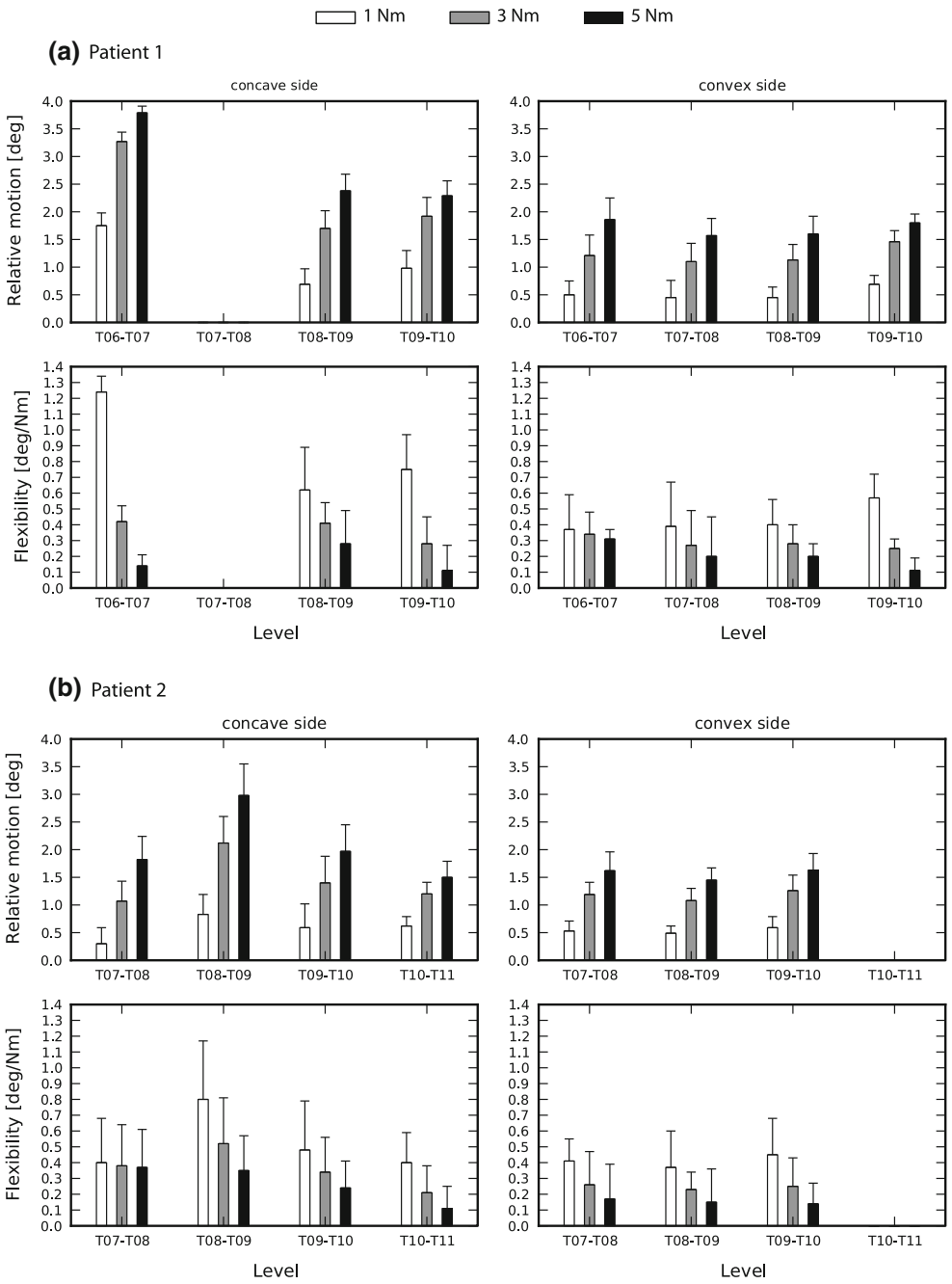

Fig. 4 Relative motion and flexibility of the four motion segments of each patient for applied lateral bending moments of 1, 3, and 5 N m. The given values are based on fitting Eq. 1 to the loading paths of each load cycle. Mean values and standard deviations are based on load cycles two to four of each segment

the motion segment. Third, while the range of motion in lateral bending was between 4° and 6° in the validation study, intraoperatively only 2°−4° were measured. A smaller range of motion increases the stochastic errors of the orientation and the position of the axis of rotation.

During the measurements, the patients were in a prone position and anesthetized. Thus, less axial compressive preload as in the upright position was present. However, the surrounding anatomical structures, especially the rib cage, constrained the motion of the vertebral column. This means that the measurements include the stiffness of the intervertebral disc, ligaments, facet joints, capsules and the costovertebral joints.

To the best of our knowledge, no in vivo intraoperative measurements to determine moment–angle relations of thoracic motion segments have yet been made. Values for

segmental flexibility could only be compared to experiments with straight cadaver spines that were obtained from middle-aged or elderly people. Panjabi et al. [19] tested single segments with a mean age of 42 years with intact costovertebral joins and no axial preload. Mean flexibility values of all motion segments were presented at a load of 5 N m, as no trend related to the level of the spine could be identified. The flexibility of the thoracic spine in right lateral bending was 0.385 and 0.33°/N m in left lateral bending. The average flexibility at a load of 5 N m in our study was 0.18 ± 0.08°/N m on the convex side, which corresponds to left lateral bending, and 0.24 ± 0.11°/N m on the concave side, which corresponds to right lateral bending (Table 2). Flexibility was lower in our study than that of Panjabi et al., which can be explained by the constraints imposed by the surrounding anatomical structures, particularly the rib cage.

Busscher et al. [2] studied multilevel segments of the thoracolumbar spine with intact costovertebral joints in patients of mean age 72 years. An axial preload of 250 N was applied to simulate the physiological condition of standing upright. Flexibility was determined as the slope in the moment–angle diagram between 3.5 and 4 N m. Flexibility of 0.19 ± 0.36°/N m was reported for the middle of the T05–T07 segment and 0.16 ± 0.1°/N m was reported for the middle of the T09–T12 segment. Determining the flexibility in the same way and calculating the average of all motion segments, our study yields a flexibility of 0.24 ± 0.11°/N m for the convex side and of 0.31 ± 0.1°/N m for the concave side (Table 2). Results of both studies are in agreement with the findings observed by Tawackoli et al. [24], who concluded that the flexibility of spinal segments decreased with an increasing preload.

Sran et al. [23] took cadaver specimens from T05 to T08 with a mean age of 81 years and applied pure moments of 4 N m in the main anatomical directions. No axial preload was reported and the ribs were completely removed. Sran et al. determined flexibility by calculating the linear regression line of the loading parts in each direction. For the mean of the T05–T06, T06–T07 and T07–T08 segments, they reported a value for flexibility of 0.43 ± 0.25°/N m. On comparing our result to that of Sran et al. [23], the flexibility was determined analogously. The flexibility of the concave side was 0.54 ± 0.17°/N m and that of the convex side was 0.35 ± 0.04°/N m (Table 2). This comparison again shows higher flexibility of the concave side. The mean value of the two sides was 0.45 ± 0.15°/N m.

Various studies confirm differing stiffness of the two sides of the scoliotic curve. Lafon et al. [16] determined the spinal intervertebral stiffness with an inverse approach based on radiographs in an upright position and after lateral bending of the patient to the left and the right sides. In a cohort of 30 patients, after the optimization, the stiffness was greater on the convex side than the concave. Duance et al. [4] performed a biochemical study to determine the collagen cross-links profile in intervertebral discs. They reported that a significantly higher level of reducible cross-links were found on the convex side, which is anticipated to result in increased stiffness in scoliosis.

The results of this study were based on seven measurements, which were performed on two patients at both sides of the spine, which limits general conclusions. However, these preliminary data show the feasibility of intraoperative, navigated distractor measurements. The results are in the same order of magnitude as existing in vitro experiments from straight spines, indicating an asymmetric flexibility between the convex and concave sides. As the study was performed on thoracic segments, the flexibility of the discoligamentous apparatus including the influence of the costovertebral joints and the rib cage was determined. The determination of moment–angle relations has distinct advantages compared to force–displacement measurements. Decoupled moment–angle relations can be compared to existing in vitro measurements, which helps to improve the understanding of spine biomechanics. The recorded motion data of the vertebrae

Table 2 Comparison of the current study to published experimental data for the thoracic spine

Previous study by	For segment(s)	Flexibility given at bending moment (N m)	Mean value (°/N m)	Flexibility of current study (°/N m)	
				Concave side	Convex side
Panjabi et al. [18]	T01–T02, T02–T03,	5.0	0.36	0.24 ± 0.11	0.18 ± 0.08
No axial preload	T03–T04, …, T11–T12				
Busscher et al. [2]	Middle of T05–T08	Secant stiffness b/t 3.5 and 4.0	0.19 ± 0.36		
250 N preload	Middle of T09–T12	Secant stiffness b/t 3.5 and 4.0	0.16 ± 0.10	0.31 ± 0.10	0.24 ± 0.11
Sran et al. [23]	T05–T06, T06–T07,	Lin. reg. b/t −4.0 and 4.0			
No axial prelaod	T07–T08		0.43 ± 0.25	0.54 ± 0.17	0.35 ± 0.04

Flexibility in the current study was determined at the same load and using the same method as the published results. The results of the current study are the mean flexibility values of all measurements of both patients on the convex and concave sides. Flexibility values are given in mean ± SD (where available)

provide information on the coupling behavior of the segment. Furthermore, the proposed technique provides the surgeon a better picture of the patient's condition. The data can be used for numerical models considering patient-specific geometry and mechanical properties. Such models would be helpful for the development of new implant designs and treatment strategies.

Acknowledgments This research has been supported by NCCR Co-Me of the Swiss National Science Foundation.

Conflict of interest None.

References

1. Brown MD, Holmes DC, Heiner AD, Wehman KF (2002) Intraoperative measurement of lumbar spine motion segment stiffness. Spine (Phila Pa 1976) 27(9):954–958
2. Busscher I, van Dieën JH, Kingma I, van der Veen AJ, Verkerke GJ, Veldhuizen AG (2009) Biomechanical characteristics of different regions of the human spine: an in vitro study on multilevel spinal segments. Spine (Phila Pa 1976) 34(26):2858–2864
3. Chang LY, Pollard NS (2007) Robust estimation of dominant axis of rotation. J Biomech 40(12):2707–2715
4. Duance VC, Crean JK, Sims TJ, Avery N, Smith S, Menage J, Eisenstein SM, Roberts S (1998) Changes in collagen cross-linking in degenerative disc disease and scoliosis. Spine (Phila Pa 1976) 23(23):2545–2551
5. Ebara S, Harada T, Hosono N, Inoue M, Tanaka M, Morimoto Y, Ono K (1992) Intraoperative measurement of lumbar spinal instability. Spine (Phila Pa 1976) 17(3 Suppl):S44–S50
6. Eguizabal J, Tufaga M, Scheer JK, Ames C, Lotz JC, Buckley JM (2010) Pure moment testing for spinal biomechanics applications: fixed versus sliding ring cable-driven test designs. J Biomech 43(7):1422–1425
7. Gédet P, Thistlethwaite PA, Ferguson SJ (2007) Minimizing errors during in vitro testing of multisegmental spine specimens: considerations for component selection and kinematic measurement. J Biomech 40(8):1881–1885
8. Ghiselli G, Wang JC, Bhatia NN, Hsu WK, Dawson EG (2004) Adjacent segment degeneration in the lumbar spine. J Bone Joint Surg Am 86-A(7):1497–1503
9. Ghista DN, Viviani GR, Subbaraj K, Lozada PJ, Srinivasan TM, Barnes G (1988) Biomechanical basis of optimal scoliosis surgical correction. J Biomech 21(2):77–88
10. Goffin J, Geusens E, Vantomme N, Quintens E, Waerzeggers Y, Depreitere B, Calenbergh FV, van Loon J (2004) Long-term follow-up after interbody fusion of the cervical spine. J Spinal Disord Tech 17(2):79–85
11. Guan Y, Yoganandan N, Moore J, Pintar FA, Zhang J, Maiman DJ, Laud P (2007) Moment–rotation responses of the human lumbosacral spinal column. J Biomech 40(9):1975–1980
12. Hasegewa K, Kitahara K, Hara T, T K, Shimoda H (2009) Biomechanical evaluation of segmental instability in degenerative lumbar spondylolisthesis. Eur Spine J 18(4):465–470
13. Heuer F, Schmidt H, Claes L, Wilke HJ (2007) Stepwise reduction of functional spinal structures increase vertebral translation and intradiscal pressure. J Biomech 40(4):795–803
14. Heuer F, Schmidt H, Klezl Z, Claes L, Wilke HJ (2007) Stepwise reduction of functional spinal structures increase range of motion and change lordosis angle. J Biomech 40(2):271–280
15. Krenn MH, Ambrosetti-Giudici S, Pfenniger A, Burger J, Piotrowski WP (2008) Minimally invasive intraoperative stiffness measurement of lumbar spinal motion segments. Neurosurgery 63(4 Suppl 2):309–313 (discussion 313–4)
16. Lafon Y, Lafage V, Steib JP, Dubousset J, Skalli W (2010) In vivo distribution of spinal intervertebral stiffness based on clinical flexibility tests. Spine (Phila Pa 1976) 35(2):186–193
17. Oxland TR, Lin RM, Panjabi MM (1992) Three-dimensional mechanical properties of the thoracolumbar junction. J Orthop Res 10(4):573–580
18. Panjabi MM, Brand RA, White AA (1976) Mechanical properties of the human thoracic spine as shown by three-dimensional load–displacement curves. J Bone Joint Surg Am 58(5):642–652
19. Panjabi MM, Brand RA, White AA (1976) Three-dimensional flexibility and stiffness properties of the human thoracic spine. J Biomech 9(4):185–192
20. Panjabi MM, Oxland TR, Yamamoto I, Crisco JJ (1994) Mechanical behavior of the human lumbar and lumbosacral spine as shown by three-dimensional load–displacement curves. J Bone Joint Surg Am 76(3):413–424
21. Petit Y, Aubin CE, Labelle H (2004) Patient-specific mechanical properties of a flexible multi-body model of the scoliotic spine. Med Biol Eng Comput 42(1):55–60
22. Reutlinger C, Gédet P, Büchler P, Kowal J, Rudolph T, Burger J, Scheffler K, Hasler C (2011) Combining 3D tracking and surgical instrumentation to determine the stiffness of spinal motion segments: a validation study. Med Eng Phys 33(3):340–346
23. Sran MM, Khan KM, Zhu Q, Oxland TR (2005) Posteroanterior stiffness predicts sagittal plane midthoracic range of motion and three-dimensional flexibility in cadaveric spine segments. Clin Biomech (Bristol, Avon) 20(8):806–812
24. Tawackoli W, Marco R, Liebschner MAK (2004) The effect of compressive axial preload on the flexibility of the thoracolumbar spine. Spine (Phila Pa 1976) 29(9):988–993
25. Wilke HJ, Claes L, Schmitt H, Wolf S (1994) A universal spine tester for in vitro experiments with muscle force simulation. Eur Spine J 3(2):91–97
26. Yamamoto I, Panjabi MM, Crisco T, Oxland T (1989) Three-dimensional movements of the whole lumbar spine and lumbosacral joint. Spine (Phila Pa 1976) 14(11):1256–1260